Transmit Beamforming for MIMO Dual Functional Radar-Communication with IQI

Junqiu Wang, Yunfei Chen, *Senior Member, IEEE* , Li Chen

***Abstract*—Multiple-input-multiple-output (MIMO) dual-functional radar communication (DFRC) provides a solution to the severe spectrum scarcity challenge. MIMO systems may be prone to the hardware impairments (HWI). Considering I/Q-imbalance (IQI), the most common type of HWI, we study the optimal transmit beamforming design for MIMO DFRC. Both radar-centric and communication-centric scenarios are investigated. For the radar-centric design, the radar beampattern and communciations user signal-to-interference-plus-noise ratio (SINR) with IQI are derived. Then, the radar beampattern is optimized by using the semidefinite relaxation (SDR) method. For the communication-centric design, the achievable rate with IQI is derived. Then, the transmit beamforming is optimized with the constraint on the MIMO radar receive signal-to-noise ratio (SNR). Moreover, the computational complexity is analyzed. Numerical results verify that IQI amplitude mismatch, IQI phase mismatch and the IQI mitigation error can significantly degrade the system's overall performance. Also, for the communication-centric scenario, IQI phase mismatch at the CUs is much more important than that at the BS.**

***Index Terms*—Achievable rate, beamforming, beampattern, dual-functional radar-communication, I/Q imbalance, zero-forcing.**

I. Introduction

In the upcoming sixth-generation (6G) era, there will be a massive number of connected devices, which will require much more spectrum resources for operation. These requirements will impose a serious challenge on spectrum scarcity to limit the overall throughput of the communications systems [1]. To alleviate this problem, joint radar and communications systems (JRC) have been proposed, allowing a variety of radar systems to share their spectrum with wireless communications systems [2]. In particular, various dual-functional systems have been proposed [3].

Due to the inevitable limitations of traditional single-antenna systems, multiple-input-multiple-output (MIMO) dual-functional radar and communication (DFRC) has been extensively studied. One major approach to achieve MIMO DFRC is to design the waveform of the transmitted signals. The closed-form globally optimal waveform designs for both omnidirectional and directional cases were obtained, and a weighted optimization was solved by a branch-and-bound algorithm under constant waveform modulus constraint in [4]. A new technique for DFRC system enabling both sidelobe control of the transmit beamforming and waveform diversity was proposed to deliver information to multiple communication directions outside the radar's mainlobe [5]. The subcarrier power in the waveform design problem for an orthogonal frequency division multiplexing (OFDM) DFRC system was studied in [6]. Considering the range sidelobe control, a novel waveform design was proposed for MIMO DFRC system [7]. The authors in [8] investigated the joint waveform design and passive beamforming in reconfigurable intelligent surface (RIS) assisted DFRC system to mitigate the high multi-user interference caused by the limited degrees of freedom of the waveform design.

In addition to waveforms, beamforming is also an efficient approach to achieve MIMO DFRC. The MIMO DFRC beamforming designs were studied to simultaneously detect radar targets and communicate with downlink communication with imperfect channel state information by maximizing the radar output power subject to probabilistic outage signal-to-interference-and-noise ratio (SINR) constraints in [9]. A novel consensus alternating direction method of multipliers approach was proposed to deploy hybrid beamforming (HBF) for OFDM-DFRC system [10]. Another HBF design along with direction-of-arrival estimation was proposed in multi-carrier DFRC systems to minimize the mean squared error between the generated spatial spectrum and the reference one under constraints of constant waveform modulus, communication quality of service and power as well as orthogonality [11]. For millimeter wave MIMO DFRC scenario, a novel HBF was studied to minimize the gap between the realized radar beam pattern and the objective, which was subject to constraints of the total DFRC transmission power and the SINR of CU [12]. The work of [13] proposed a joint design of transmit beamforming and receive filters for a coordinated two-cell network by formulating the non-convex optimization problem of minimizing the transmit power at two base stations (BSs) under SINR constraints. The authors in [14] investigated a DFRC scheme combining degrees of freedom in frequency and space to deliver digital information via index modulation. Beamforming has also been found to improve the security performance for MIMO DFRC systems. For example, the joint transmit waveform and receive beamforming design was proposed to maximize the radar SINR under the constraints of security and power budget when the radar target might

This work was supported in part by the King Abdullah University of Science and Technology Research Funding (KRF) under Award ORA-2021-CRG10-4696.

Junqiu Wang is with the School of Engineering, University of Warwick, Coventry, UK CV4 7AL (e-mail:Qiuqiu.Wang@warwick.ac.uk).

Yunfei Chen is with Department of Engineering, University of Durham, Durham, UK DH1 3LE (e-mail: Yunfei.Chen@durham.ac.uk).

Li Chen is with the CAS Key Laboratory of Wireless-Optical Communications, University of Science and Technology of China, Hefei 101127, China (e-mail: chenli87@ustc.edu.cn).

be a potential eavesdropper [15]. The transmit beamforming was designed to maximize the sum secrecy rate for more CUs leveraged by non-orthogonal multiple access in [16]. Taking account of the physical layer security, a novel beamforming scheme was proposed and indicated that the corresponding DFRC radar waveforms could be regarded as the traditional artificial noise that was exploited for improved degrees of freedom and for drowning out the eavesdropping channel [17].

Moreover, DFRC has been incorporated in other 6G technologies. In vehicle to everything, DFRC technique was employed to investigate a radar-assisted predictive beamforming design [18]. The authors in [19] proposed an innovative single-target-multi-beam radar beam alignment approach to mitigate inter-radar interference in vehicle-to-everything systems using DFRC. A novel DFRC cooperative sensing unmanned aerial vehicle network was designed to enhance the cooperative sensing ability [20]. For edge computing, [21] created an DFRC based integrated architecture of communication, sensing and mobile-edge computing to perform radar detection and computation offloading simultaneously at the user terminals. The joint optimization of the RIS passive phase-shift matrix and transmit beamforming was studied to enhance the radar performance where the target was within a crowded area [22]. Joint DFRC waveform, passive beamforming and RIS phase shift matrix were optimized in the RIS-assisted DFRC system to minimize multi-user interference under the strict beampattern constraint [23].

On the other hand, low cost hardware components are widely used, in particular in MIMO radar and MIMO communications systems, to reduce the overall cost of the system. Both communications and radar performance are largely affected by hardware impairment (HWI) since these HWI will cause phase and amplitude mismatch, raise noise floor or distort image signals [24]. In-phase/quadrature imbalance (IQI) is one of the most common HWI types which has been extensively studied during the past decade. In an OFDM system with maximum ratio combining detection, the analytical outage probability of half-duplex amplify-and-forward relaying with IQI was derived [25]. The authors in [26] derived the outage probability's exact and tight analytical lower bounds over independent and non-identically distributed Nakagamim fading channels as well as the tractable upper and lower bounds on the ergodic capacity in the presence of IQI with arbitrary SNR [26]. The work of [27] considered both IQI and additive distortion to derive the outage probabilities of both amplify-and-forward and decode-and-forward relaying schemes and analyze their performances. A low-complexity joint analog and digital self-interference cancellation approach for the full duplex transceiver with IQI was proposed [28].

Besides IQI, other HWI types, such as power amplifier non-linearity, phase noise and carrier frequency offset may also occur. For instance, the compensation method of the power amplifier nonlinearity was proposed in large-scale multi-user MIMO downlink systems [29]. The authors in [30] studied the effect of power amplifier non-linearity on the closed form expressions for achievable sum-rate. The work of [31] exploited location-specific channel gain and transmitter-specific phase noise which were two intrinsic physical-layer features for massive MIMO. Considering phase noise at both transmitter and receiver, the compensation scheme for such practical imperfections in high-mobility scenarios was proposed for the non-stationary and time-varying millimeter wave MIMO communication systems [32]. Closed-form expressions of achievable rate were derived considering quasi-static radio frequency mismatch, channel estimation error and carrier frequency offset [33]. The achievable downlink sum-rate of massive MIMO system was derived [34].

All the above works have provided helpful insights on DFRC or HWI. Nevertheless, to the best of our knowledge, none has considered HWI in DFRC designs. Motivated by the above observation, in this work, we study a beamforming design for the DFRC system that simultaneously detects the target as a MIMO radar and communicates with multiple communications users by considering the effect of IQI. We first formulate the radar-centric transmit beamforming problem to optimally design the radar beampattern while guaranteeing the minimum SINR of each communications user. The radar performance metric and communications performance metric are derived in the presence of IQI. Due to the non-convex constraint, semidefinite relaxation (SDR) approximation is used to solve the optimization problem. For the communication-centric transmit beamforming problem, the achievable rate with IQI is derived. To reduce the optimization complexity, a zero-forcing beamforming method is used. The MIMO radar receiving SNR is calculated as the performance constraint of the radar function. Then, the communication-centric transmit beamforming problem is formulated and solved. In summary, the main contributions of our work are as follows:

1) We consider HWI in the DFRC beamforming architecture that has been ignored in the previous works.
2) We propose a radar-centric beamforming design method which combines MIMO radar beampattern with communications user SINR and is solved by using the SDR approxmation method.
3) We study a communication-centric beamforming optimization via zero-forcing beamforming method to maximize the communications rate with constraint on the MIMO radar receiving SNR.
4) We demonstrate that both IQI parameters and IQI mitigation have significant impact on the DFRC performance. Also, IQI phase mismatch at the CUs has more significant impact than IQI phase mismatch at the BS for the communication-centric problem when they are of asymmetric levels.

The remainder of this paper is organized as follows. Section II presents the system model with IQI. Sections III and Section IV study the radar-centric beamforming problem and communication-centric beamforming problem, respectively. Simulation results and discussion are provided in Section V. Finally, conclusions are made in Section VI.

Notations: The italic letter denotes a scalar and the lower case boldface letter represents a vector. $\mathcal{CN}(a, b, c)$ denotes a complex Gaussian random variable with mean a, variance b and pseudo variance c. $\mathrm{E}(\cdot)$ represents the expectation operation. Superscripts $()^H$ and $()^T$ stand for Hermitian

transpose and transpose, respectively. $tr()$, $diag()$, and $rank()$ represent the trace operation, the vector formed by the diagonal elements and the rank operator, respectively. $\mathcal{C}^{m\times n}$ is the set of complex-valued $m \times n$ matrices.

II. SYSTEM MODEL

The DFRC BS has N_t transmit antennas to serve K single-antenna communication users (CUs) indexed by $k \in \{1, \cdots, K\}$. The DFRC BS also operates as a MIMO radar so that it has N_r receive antennas for receiving the return radar signal. Thus, the BS waveform transmission and echo reception are not time divisioned but instead simultaneously on two sets of antenna. Consequently, no full-duplex mode is needed. For convenience, we let $N_t = N_r = N$. The transmitted signal vector $\mathbf{c} = [c_1, c_2, ..., c_K]^T \in \mathcal{C}^{K\times 1}$ at BS are the dual-functional waveforms where the element c_k of $\mathbf{c}$ is simultaneously intended for the k-th CU as the communications symbols and for radar probing. The dual-functional waveforms $\mathbf{c}$ is precoded by the transmit beamforming matrix $\mathbf{B} \triangleq [\mathbf{B}_1, ..., \mathbf{B}_K] \in \mathcal{C}^{N\times K}$ where $\mathbf{B}_k \in \mathcal{C}^{N\times 1}$ is the precoder for c_k. The goal of our work is to design $\mathbf{B}$ with the following assumptions: 1) each c_k has zero-mean and they are uncorrelated with each other with $\mathbf{c} \sim \mathcal{CN}(\mathbf{0}, \mathbf{I_K}, \mathbf{0})$; 2) $\mathbf{H} \triangleq [\mathbf{h}_1, ..., \mathbf{h}_K] \in \mathcal{C}^{N\times K}$ is the flat Rayleigh fading instantaneous downlink channel matrix where $\mathbf{h}_k \in \mathcal{C}^{N\times 1}$ is the physical channel vector between the BS antennas and the k-th CU, and $\mathbf{H}$ remains unchanged during one transmission; 3) the transmitter has knowledge of $\mathbf{H}$ obtained by exploiting wireless channel reciprocity via uplink channel estimation in a time-division duplex mode [35], [36].

A. Receiced Signal at the CUs

After precoding, the $\mathcal{C}^{N\times 1}$ signal transmitted by the BS is given as

$$\mathbf{x} = \mathbf{Bc}. \tag{1}$$

For the i-th antenna at the BS, the IQI coefficient is denoted as $G_{1,i} = \frac{1+g_{T,i}e^{\phi_{T,i}}}{2}$ and $G_{2,i} = \frac{1-g_{T,i}e^{-\phi_{T,i}}}{2}$ where $g_{T,i}$ and $\phi_{T,i}$ are the amplitude mismatch and phase mismatch for BS antenna i, respectively. By denoting the BS IQI coefficient in a diagonal matrix $\mathrm{diag}(G_{1,1}, ..., G_{1,N}) \in \mathcal{C}^{N\times N}$ as $\mathbf{G_1}$ and $\mathrm{diag}(G_{2,1}, ..., G_{2,N}) \in \mathcal{C}^{N\times N}$ as $\mathbf{G_2}$, the IQI distorted transmitted symbol at the BS is

$$\mathbf{x}_T = \mathbf{G}_1\mathbf{x} + \mathbf{G}_2^*\mathbf{x}^*. \tag{2}$$

Let the symbols received at the CUs be

$$\mathbf{x_R} = \mathbf{H}^T\mathbf{x}_T + \mathbf{n} \tag{3}$$

where $\mathbf{n} \triangleq [n_1, ..., n_K]^T$ is the additive white Gaussian noise (AWGN) vector with $\mathbf{n} \sim \mathcal{CN}(\mathbf{0}, \mathbf{I_K}, \mathbf{0})$. At the receivers for the CUs, there also exists IQI as $K_{1,k} = \frac{1+g_{R,k}e^{-\phi_{R,k}}}{2}$ and $K_{2,k} = \frac{1-g_{R,k}e^{\phi_{R,k}}}{2}$ where $g_{R,k}$ and $\phi_{R,k}$ are the amplitude mismatch and phase mismatch at the k-th CU, respectively. Similarly, using the diagonal matrix $\mathbf{K_1} \in \mathcal{C}^{K\times 1}$ and $\mathbf{K_2} \in \mathcal{C}^{K\times 1}$, the distorted received signal at the CU is

$$\mathbf{y} = \mathbf{K}_1\mathbf{x}_R + \mathbf{K}_2\mathbf{x}_R^*. \tag{4}$$

Substituting (1), (2) and (3) into (4), one has

$$\begin{aligned}\mathbf{y} =&(\mathbf{K}_1\mathbf{H}^T\mathbf{G}_1 + \mathbf{K}_2\mathbf{H}^H\mathbf{G}_2)\mathbf{Bc} + (\mathbf{K}_1\mathbf{H}^T\mathbf{G}_2^* + \mathbf{K}_2\mathbf{H}^H\mathbf{G}_1^*)\mathbf{B}^*\mathbf{c}^* \\ &+ \mathbf{K}_1\mathbf{n} + \mathbf{K}_2\mathbf{n}^*.\end{aligned} \tag{5}$$

For simplicity, we denote $(\mathbf{K}_1\mathbf{H}^T\mathbf{G}_1 + \mathbf{K}_2\mathbf{H}^H\mathbf{G}_2)$ as the effective channel $\mathbf{H}_1^T$ where $\mathbf{H}_1 \triangleq [\mathbf{h}_{11}, ..., \mathbf{h}_{1K}]$ with $\mathbf{h}_{1k} \in \mathcal{C}^{N\times 1}$ being the effective channel vector between the BS antennas and the k-th CU. Similarly, we denote $\mathbf{K}_1\mathbf{H}^T\mathbf{G}_2^* + \mathbf{K}_2\mathbf{H}^H\mathbf{G}_1^*$ as the effective IQI channel $\mathbf{H}_2^T \triangleq [\mathbf{h}_{21}, ..., \mathbf{h}_{2K}]$. Therefore, (5) is simplified as

$$\mathbf{y} = \mathbf{H}_1^T\mathbf{Bc} + \mathbf{H}_2^T\mathbf{B}^*\mathbf{c}^* + \mathbf{z} \tag{6}$$

where $\mathbf{z} = \mathbf{K}_1\mathbf{n} + \mathbf{K}_2\mathbf{n}^*$ and $\mathbf{z}$ is improper Gaussian due to the introduction of $\mathbf{n}^*$ term.

B. MIMO Radar Receiving Signal

Meanwhile, the IQI distorted transmitted signal $\mathbf{x}_T$ at the BS is also used for radar detection. Given the transmit signal $\mathbf{x}_T$ in (2), the echo signal received by another set of antennas at the radar receiver is

$$\begin{aligned}\mathbf{y}_0 &= \alpha_0\mathbf{a}_r(\theta)\,\mathbf{a}_t^T(\theta)\,\mathbf{x}_T + \mathbf{n}_0 \\ &= \alpha_0\mathbf{A}(\theta)\,\mathbf{x}_T + \mathbf{n}_0\end{aligned} \tag{7}$$

where α_0 is the complex amplitude proportional to the radar cross section (RCS) of the target [37], [38], θ denotes the target direction, $\mathbf{a}_t(\theta) = \mathbf{a}_r(\theta) \triangleq [1, e^{j2\pi\Delta\sin\theta}, ..., e^{j2\pi(N-1)\Delta\sin\theta}]^T$ are the steering vectors of the transmit antenna array and the receive antenna array, respectively, with Δ being the spacing between adjacent antennas normalized by the wavelength and $\mathbf{n}_0$ is the AWGN with $\mathcal{CN}(\mathbf{0}, \mathbf{I_N}, 0)$. Using linearly independent waveforms that yield linearly independent radar return signals reflected from different targets, data-dependent array algorithms, such as Capon, amplitude and phase estimation (APES) and the combined method of Capon and APES (CAPES), can be employed to estimate θ and α_0 [37]. Similarly, the radar receiver has IQI, whose coefficient diagonal matrix $\mathbf{K}_{r1}$ has the i-th diagonal element as $K_{r1,i} = \frac{1+g_{r,i}e^{-\phi_{r,i}}}{2}$ where $g_{r,i}$ and $\phi_{r,i}$ are the receiving amplitude mismatch and phase mismatch at the i-th radar receiving antenna, respectively. Accordingly, $\mathbf{K}_{r2} = \mathbf{I} - \mathbf{K}_{r1}^*$. Thus, $\mathbf{y}_0$ becomes

$$\mathbf{y}_1 = \mathbf{K}_{r1}\mathbf{y}_0 + \mathbf{K}_{r2}\mathbf{y}_0^*. \tag{8}$$

The final output of the radar receiver is

$$y_r = \mathbf{w}^H\mathbf{y}_1 \tag{9}$$

where $\mathbf{w} \in \mathcal{C}^{N\times 1}$ is the radar receive beamforming vector designed to achieve the maximum output radar SNR. To further expand (9) with (8) and (7), one has

$$y_r = \mathbf{w}^H\mathbf{M}_1\mathbf{x} + \mathbf{w}^H\mathbf{M}_2\mathbf{x}^* + \mathbf{w}^H\mathbf{K}_{r1}\mathbf{n}_0 + \mathbf{w}^H\mathbf{K}_{r2}\mathbf{n}_0^* \tag{10}$$

where

$$\mathbf{M}_1 = \alpha_0\mathbf{K}_{r1}\mathbf{A}(\theta)\,\mathbf{G}_1 + \alpha_0^*\mathbf{K}_{r2}\mathbf{A}^*(\theta)\,\mathbf{G}_2 \tag{11}$$

and

$$\mathbf{M}_2 = \alpha_0\mathbf{K}_{r1}\mathbf{A}(\theta)\,\mathbf{G}_2^* + \alpha_0^*\mathbf{K}_{r2}\mathbf{A}^*(\theta)\,\mathbf{G}_1^*. \tag{12}$$

Our purpose is to optimally design the transmit precoding $\mathbf{B}$ and the radar receive beamforming vector $\mathbf{w}$.

III. Radar-centric Beamforming

The MIMO communications system exploits the spatial diversity using an array of transceive antennas and rich multipath channels to increase capacity and enhance communications performance. It requires sampling, quantization, symbol mapping, space/time encoding, RF up-conversion, matched-filtering and the corresponding inverse operations at the receiver [39]. The MIMO radar system exploits the additional spatial degrees of freedom to provide more flexible resource management, improved parameter identifiability and much better angular and range resolution [40]. It focuses on radar processing, such as matched-filtering, beamforming, Doppler detection, range detection and peak detection [41]. They have different design purposes. The proposed MIMO DFRC system uses an integrated dual-functional waveform to simultaneously communicate with multiple downlink users and detect radar targets for the tradeoff between the radar performance and the communications performance. In this section, we will consider the radar-centric beamforming design problem. The performance metrics of MIMO radar and multiuser MIMO communication with IQI will be derived in Sections III-A and III-B, respectively.

A. MIMO Radar Beampattern with IQI

For MIMO radar, its desired beamforming shall synthesize the transmit beam towards the target. Therefore, the radar beampattern is adopted as the main radar performance metric in this work to optimize the transmit beamforming [3], [42] and [43]. To calculate the transmit beampattern (transmit power) at a given angular direction θ, one first defines the radar transmit waveform covariance matrix as

$$\begin{aligned}\mathbf{R} &= \mathrm{E}(\mathbf{x_T x_T}^H) \\ &= \mathbf{G}_1(\sum_{k=1}^{K}\mathbf{B}_k\mathbf{B}_k^H)\mathbf{G}_1^* + \mathbf{G}_2^*(\sum_{k=1}^{K}\mathbf{B}_k\mathbf{B}_k^H)^*\mathbf{G}_2.\end{aligned} \tag{13}$$

The transmit beampattern for the DFRC system is [49, (10)]

$$P_d(\theta;\mathbf{R}) = \mathbf{a}_t^H(\theta)\mathbf{R}\mathbf{a}_t(\theta). \tag{14}$$

Also, from [49, (11)], the radar cross correlation pattern is

$$P_c(\theta_1,\theta_2;\mathbf{R}) = \mathbf{a}_t^H(\theta_2)\mathbf{R}\mathbf{a}_t(\theta_1), \tag{15}$$

where θ_1 and θ_2 represent different values of θ. The radar transmit waveform covariance matrix $\mathbf{R}$ determines both the transmit beam pattern and cross correlation pattern in (14) and (15). Thus, optimally designing the covariance matrix $\mathbf{R}$ is critical. In this sense, the design of beampattern is equivalent to designing the covariance matrix of the probing signals [3], [42]. To generate a beampattern with a desired 3dB main-beam width, the radar-centric beampattern problem proposed is

$$\begin{aligned}\min_{t,\mathbf{R}} \quad & -t \\ \text{s.t.} \quad & P_d(\theta_0) - P_d(\theta_m) \geq t, \quad \forall\theta_m \in \Omega, \\ & P_d(\theta_1) - P_d(\theta_0)/2 = 0, \\ & P_d(\theta_2) - P_d(\theta_0)/2 = 0, \\ & \mathbf{R} \succeq 0, \mathbf{R} = \mathbf{R}^H, \\ & [\mathbf{R}]_{m,m} = \tfrac{P_t}{N}, \forall m = 1,2,...,N\end{aligned} \tag{16}$$

where θ_0 is the location of the main-beam, $(\theta_2 - \theta_1)$ determines the 3dB mainlobe beam width, Ω denotes the sidelobe region and P_t is the total transmit power. This is the conventional convex optimization problem studied in [43] and will be used as a benchmark radar beampattern.

B. Multiuser MIMO Communication SINR

For multiuser MIMO communication, the precoder is designed to guarantee the minimum receiving SINR at each CU. In multiuser transmit beamforming, the precoder should be designed to guarantee a certain level of SINR at the users. Here, it is assumed that the transmitter has knowledge of the instantaneous downlink channel H. This knowledge can be obtained, for example, by exploiting wireless channel reciprocity when operating in time-division duplex mode, i.e., the downlink channel is obtained via uplink channel estimation. Fairness SINR, which is the lowest SINR among all communciations downlinks, is used as the performance metric for multiple CUs. It is required to be higher than a given threshold to guarantee a minimal level of communication quality of service at each user, i.e.,

$$\gamma_k \geq \Gamma, \forall k = 1,2,...,K. \tag{17}$$

For the k-th CU, from (6) one has

$$\begin{aligned}y_k &= \mathbf{h}_{1k}^T\mathbf{B}\mathbf{c} + \mathbf{h}_{2k}^T\mathbf{B}^*\mathbf{c}^* + K_{1,k}n_k + K_{2,k}n_k^* \\ &= \mathbf{h}_{1k}^T\mathbf{B}_k c_k + \underbrace{\mathbf{h}_{1k}^T\sum_{i=1,i\neq k}^{K}\mathbf{B}_i c_i + \mathbf{h}_{2k}^T\sum_{i=1}^{K}\mathbf{B}_i^* c_i^*}_{①} \\ &\quad + \underbrace{K_{1,k}n_k + K_{2,k}n_k^*}_{②}\end{aligned} \tag{18}$$

where $\mathbf{h}_{1k}^T\mathbf{B}_k c_k$ is the desired signal part, ① is the overall interference made of the multi-user interference in the first part and the IQI interference in the second part [44], and ② is the noise. The interference power is

$$\begin{aligned}|①|^2 =& |\mathbf{h}_{1k}^T\sum_{i=1,i\neq k}^{K}\mathbf{B}_i c_i|^2 + |\mathbf{h}_{2k}^H\sum_{i=1}^{K}\mathbf{B}_i c_i|^2 \\ &+ 2\,\mathrm{Re}\left\{(\mathbf{h}_{1k}^T\sum_{i=1,i\neq k}^{K}\mathbf{B}_i c_i)(\mathbf{h}_{2k}^H\sum_{i=1}^{K}\mathbf{B}_i c_i)\right\}.\end{aligned} \tag{19}$$

Using assumptions on c_i, it can be obtained as

$$\mathrm{E}_{\mathbf{c}}(|①|^2) = \sum_{i=1,i\neq k}^{K}|\mathbf{h}_{1k}^T\mathbf{B}_i|^2 + \sum_{i=1}^{K}|\mathbf{h}_{2k}^H\mathbf{B}_i|^2. \tag{20}$$

Similarly, we have

$$\mathrm{E}_{\mathbf{c}}(|②|^2) = |K_{1,k}|^2 + |K_{2,k}|^2 \tag{21}$$

and

$$\mathrm{E}_{\mathbf{c}}(|\mathbf{h}_{1k}^T\mathbf{B}_k c_k|^2) = |\mathbf{h}_{1k}^T\mathbf{B}_k|^2. \tag{22}$$

The SINR γ_k at the k-th user can be calculated from (20), (21) and (22) as

$$\gamma_k = \frac{|\mathbf{h}_{1k}^T\mathbf{B}_k|^2}{\sum_{i=1,i\neq k}^{K}|\mathbf{h}_{1k}^T\mathbf{B}_i|^2 + \sum_{i=1}^{K}|\mathbf{h}_{2k}^H\mathbf{B}_i|^2 + |K_{1,k}|^2 + |K_{2,k}|^2}. \tag{23}$$

Algorithm 1 Radar-Centric Optimization via SDR

1: Remove the constraint '$\mathrm{rank}(\mathbf{R_k}) = 1$' in (27g) of the initial problem (27) to obtain the SDR convex problem (28).
2: Solve (28) and obtain the solutions of (28) as $\widetilde{\mathbf{R}}_0, \widetilde{\mathbf{R}}_1, ..., \widetilde{\mathbf{R}}_K$.
3: Compute $\hat{\mathbf{B}}_k$ for each k by (29).
4: Set the overall beamforming matrix $\hat{\mathbf{B}}$ as $[\hat{\mathbf{B}}_1, ..., \hat{\mathbf{B}}_K]$.

C. Problem Formation and Solution

The goal of radar-centric DFRC beamforming is to optimize the radar beam pattern with constraints on the transmit power and communication quality of service. Therefore, we establish the radar-centric optimization problem to minimize the loss function on radar beam pattern defined in (16), with the per-antenna power constraint and the fairness SINR constraint (17) for each downlink user as

$$\begin{aligned} \min_{t,\mathbf{R}} \quad & -t \\ \text{s.t.} \quad & P_d(\theta_0) - P_d(\theta_m) \geq t, \quad \forall \theta_m \in \Omega, \\ & P_d(\theta_1) - P_d(\theta_0)/2 = 0, \\ & P_d(\theta_2) - P_d(\theta_0)/2 = 0, \\ & \mathbf{R} \succeq 0, \mathbf{R} = \mathbf{R}^H, \\ & [\mathbf{R}]_{m,m} = \tfrac{P_t}{N}, \forall m = 1, 2, ..., N, \\ & \mathbf{R} = \mathbf{G}_1(\textstyle\sum_{k=1}^{K} \mathbf{B}_k \mathbf{B}_k^H)\mathbf{G}_1^* + \mathbf{G}_2^*(\sum_{k=1}^{K} \mathbf{B}_k \mathbf{B}_k^H)^* \mathbf{G}_2, \\ & \gamma_k \geq \Gamma, \forall k = 1, 2, ..., K. \end{aligned} \tag{24}$$

Denote $\mathbf{R_k} = \mathbf{B}_k \mathbf{B}_k^H, \forall k = 1, 2, ..., K$ and $\mathbf{R_0} = \sum_{k=1}^{K} \mathbf{R_k}$, then one has

$$\begin{aligned} \gamma_k &= \frac{\mathbf{h}_{1k}^T \mathbf{R_k} \mathbf{h}_{1k}^*}{\sum_{i=1, i\neq k}^{K} \mathbf{h}_{1k}^T \mathbf{R_i} \mathbf{h}_{1k}^* + \sum_{i=1}^{K} \mathbf{h}_{2k}^H \mathbf{R_i} \mathbf{h}_{2k} + |K_{1,k}|^2 + |K_{2,k}|^2} \\ &= \frac{\mathbf{h}_{1k}^T \mathbf{R_k} \mathbf{h}_{1k}^*}{\mathbf{h}_{1k}^T \mathbf{R_0} \mathbf{h}_{1k}^* - \mathbf{h}_{1k}^T \mathbf{R_k} \mathbf{h}_{1k}^* + \mathbf{h}_{2k}^H \mathbf{R_0} \mathbf{h}_{2k} + |K_{1,k}|^2 + |K_{2,k}|^2}. \end{aligned} \tag{25}$$

From (25), one can rewrite (17) as

$$(1+\Gamma^{-1}) \mathbf{h}_{1k}^T \mathbf{R_k} \mathbf{h}_{1k}^* \geq \mathbf{h}_{1k}^T \mathbf{R_0} \mathbf{h}_{1k}^* + \mathbf{h}_{2k}^H \mathbf{R_0} \mathbf{h}_{2k} + |K_{1,k}|^2 + |K_{2,k}|^2. \tag{26}$$

Thus, (24) becomes

$$\min_{t, \mathbf{R_0}, \mathbf{R_1}, ... \mathbf{R_K}} \quad -t \tag{27a}$$
$$\text{s.t. } P_d(\theta_0) - P_d(\theta_m) \geq t, \quad \forall \theta_m \in \Omega, \tag{27b}$$
$$P_d(\theta_1) - P_d(\theta_0)/2 = 0, \tag{27c}$$
$$P_d(\theta_2) - P_d(\theta_0)/2 = 0, \tag{27d}$$
$$\mathbf{R_0} = \sum_{k=1}^{K} \mathbf{R_k}, \tag{27e}$$
$$[\mathbf{G}_1 \mathbf{R_0} \mathbf{G}_1^* + \mathbf{G}_2^* \mathbf{R_0}^* \mathbf{G}_2]_{m,m} = \frac{P_t}{N}, \forall m = 1, 2, ..., N, \tag{27f}$$
$$\mathbf{R_k} \succeq 0, \mathrm{rank}(\mathbf{R_k}) = 1, \forall k = 1, 2, ..., K, \tag{27g}$$
$$(1 + \Gamma^{-1}) \mathbf{h}_{1k}^T \mathbf{R_k} \mathbf{h}_{1k}^* \geq \mathbf{h}_{1k}^T \mathbf{R_0} \mathbf{h}_{1k}^* + \mathbf{h}_{2k}^H \mathbf{R_0} \mathbf{h}_{2k} + |K_{1,k}|^2 + |K_{2,k}|^2. \tag{27h}$$

However, the optimization problem (27) is non-convex because of the rank-one constraints in (27g). To make it convex, these constraints can be dropped, leading to the following semidefinite relaxation (SDR) problem as an approximation to (27) as

$$\min_{t, \mathbf{R_0}, \mathbf{R_1}, ... \mathbf{R_K}} \quad -t \tag{28a}$$
$$\text{s.t. } P_d(\theta_0) - P_d(\theta_m) \geq t, \quad \forall \theta_m \in \Omega, \tag{28b}$$
$$P_d(\theta_1) - P_d(\theta_0)/2 = 0, \tag{28c}$$
$$P_d(\theta_2) - P_d(\theta_0)/2 = 0, \tag{28d}$$
$$\mathbf{R_0} = \sum_{k=1}^{K} \mathbf{R_k}, \tag{28e}$$
$$[\mathbf{G}_1 \mathbf{R_0} \mathbf{G}_1^* + \mathbf{G}_2^* \mathbf{R_0}^* \mathbf{G}_2]_{m,m} = \frac{P_t}{N}, \forall m = 1, 2, ..., N, \tag{28f}$$
$$\mathbf{R_k} \succeq 0, \forall k = 1, 2, ..., K, \tag{28g}$$
$$(1 + \Gamma^{-1}) \mathbf{h}_{1k}^T \mathbf{R_k} \mathbf{h}_{1k}^* \geq \mathbf{h}_{1k}^T \mathbf{R_0} \mathbf{h}_{1k}^* + \mathbf{h}_{2k}^H \mathbf{R_0} \mathbf{h}_{2k} + |K_{1,k}|^2 + |K_{2,k}|^2. \tag{28h}$$

Each part of (28) is either linear or semidefinite so (28) is a convex problem which can be solved by using the MATLAB CVX tools [45], [46]. Denote the solutions to the approximated optimization problem in (28) as $\widetilde{\mathbf{R}}_0, \widetilde{\mathbf{R}}_1, ..., \widetilde{\mathbf{R}}_K$ (they do not have analytical expressions.). If these solutions to (28) are exactly rank-one, they are also the optimal solutions to the original non-convex problem in (27). However, if they are not exactly rank-one and the SDR problem in (28) is not tight, following the method used in [49, (32) and (33)], the solutions to the original non-convex problem in (27) can be calculated and approximated by using the solutions to (28) as the following

$$\hat{\mathbf{B}}_k = (\mathbf{h}_{1k}^T \widetilde{\mathbf{R}}_k \mathbf{h}_{1k}^*)^{-1/2} \widetilde{\mathbf{R}}_k \mathbf{h}_{1k}^*, \tag{29}$$

$$\hat{\mathbf{R}}_k = \hat{\mathbf{B}}_k \hat{\mathbf{B}}_k^H \tag{30}$$

and

$$\hat{\mathbf{R}}_0 = \sum_{k=1}^{K} \hat{\mathbf{R}}_k. \tag{31}$$

From (29) and (30), one has

$$\mathrm{rank}(\hat{\mathbf{R}}_k) = \mathrm{rank}(\hat{\mathbf{B}}_k) = 1, \forall k = 1, 2, ..., K \tag{32}$$

and

$$\mathbf{h}_{1k}^T \hat{\mathbf{R}}_k \mathbf{h}_{1k}^* = \mathbf{h}_{1k}^T \widetilde{\mathbf{R}}_k \mathbf{h}_{1k}^*, \forall k = 1, 2, ..., K \tag{33}$$

where these new solutions used by the solutions to the SDR problem in (28) satisfy the rank-one constraint in (27g). These steps are summarized in Algorithm 1. Since it is a special case of the quadratic semidefinite programming problem, its computational complexity is $\mathcal{O}\left(K^{6.5} N^{6.5} \log(1/\epsilon)\right)$ as the worst where ϵ is the solution accuracy [39], [40]. If $\hat{\mathbf{R}}_0$ in (31) equals to $\widetilde{\mathbf{R}}_0$, then $\hat{\mathbf{R}}_0, ..., \hat{\mathbf{R}}_K$ immediately satisfy all the rest constraints of (27) and they are also the optimal solutions to (27). Their effectiveness depends on how close $\hat{\mathbf{R}}_0$ in (31) is to $\widetilde{\mathbf{R}}_0$. Therefore, they are not guaranteed to be the optimal solutions to (27) but simulation results later show that they offer good performances.

IV. Communication-Centric Beamforming

In this section, we will focus on the communication-centric design to optimize the communications performance while guaranteeing the minimal requirement on the radar performance.

A. MIMO Communications Achievable Rate with IQI

Different from the previous section, the communication-centric beamforming problem maximizes the achievable rate of the MU-MIMO communications given constraints on the MIMO radar beampattern and the transmit power budget. We will first derive the achievable rate of the communications system with IQI. Since $\mathbf{z}$ is an improper Gaussian, we have its pseudo-covariance matrix as

$$\tilde{\mathbf{C}}_{\mathbf{z}} = \mathrm{E}(\mathbf{z}\mathbf{z}^T) = \mathbf{K}_1\mathbf{K}_2^{\mathrm{T}} + \mathbf{K}_2\mathbf{K}_1^{\mathrm{T}} \tag{34}$$

and the covariance matrix as

$$\mathbf{C}_{\mathbf{z}} = \mathrm{E}(\mathbf{z}\mathbf{z}^H) = \mathbf{K}_1\mathbf{K}_1^{\mathrm{H}} + \mathbf{K}_2\mathbf{K}_2^{\mathrm{H}}. \tag{35}$$

Similarly, for $\mathbf{y}$ one has

$$\begin{cases} \tilde{\mathbf{C}}_{\mathbf{y}} = \mathrm{E}(\mathbf{y}\mathbf{y}^T) = \mathbf{H}_1^T\mathbf{B}\mathbf{B}^H\mathbf{H}_2 + \mathbf{H}_2^T(\mathbf{B}\mathbf{B}^H)^*\mathbf{H}_1 + \tilde{\mathbf{C}}_{\mathbf{z}} \\ \mathbf{C}_{\mathbf{y}} = \mathrm{E}(\mathbf{y}\mathbf{y}^H) = \mathbf{H}_1^T\mathbf{B}\mathbf{B}^H\mathbf{H}_1^* + \mathbf{H}_2^T(\mathbf{B}\mathbf{B}^H)^*\mathbf{H}_2^* + \mathbf{C}_{\mathbf{z}} \end{cases} \tag{36}$$

where $\tilde{\mathbf{C}}_{\mathbf{y}}$ is not a zero matrix so that $\mathbf{y}$ is also an improper Gaussian.

To calculate the system achievable rate, define the complex augmented random vector $\underline{\mathbf{z}}$ of $\mathbf{z}$ as $\underline{\mathbf{z}} = \left[\begin{array}{cc} \mathbf{z}^{\mathrm{T}} & \mathbf{z}^{\mathrm{H}} \end{array}\right]^{\mathrm{T}}$. The entropy of $\mathbf{z}$ is [47]

$$h(\mathbf{z}) = \frac{1}{2}\log_2\left((\pi e)^{2K}\left|\underline{\mathbf{C}_{\mathbf{z}}}\right|\right) \tag{37}$$

where $\underline{\mathbf{C}_{\mathbf{z}}}$ is defined as

$$\underline{\mathbf{C}_{\mathbf{z}}} \triangleq \mathrm{E}\left(\underline{\mathbf{z}}\underline{\mathbf{z}}^{\mathrm{H}}\right) = \left[\begin{array}{cc} \mathbf{C}_{\mathbf{z}} & \tilde{\mathbf{C}}_{\mathbf{z}} \\ \tilde{\mathbf{C}}_{\mathbf{z}}^* & \mathbf{C}_{\mathbf{z}} \end{array}\right]. \tag{38}$$

From [48], one has

$$\left|\underline{\mathbf{C}_{\mathbf{z}}}\right| = \left|\mathbf{C}_{\mathbf{z}}\right|^2\left|\mathbf{I}_K - \mathbf{C}_{\mathbf{z}}{}^{-1}\tilde{\mathbf{C}}_{\mathbf{z}}\mathbf{C}_{\mathbf{z}}{}^{-\mathrm{T}}\tilde{\mathbf{C}}_{\mathbf{z}}{}^{\mathrm{H}}\right|. \tag{39}$$

Thus, (37) becomes

$$h(\mathbf{z}) = \log_2\left((\pi e)^K\left|\mathbf{C}_{\mathbf{z}}\right|\right) + \frac{1}{2}\log_2\left|\mathbf{I}_K - \mathbf{C}_{\mathbf{z}}^{-1}\tilde{\mathbf{C}}_{\mathbf{z}}\mathbf{C}_{\mathbf{z}}^{-\mathrm{T}}\tilde{\mathbf{C}}_{\mathbf{z}}^{\mathrm{H}}\right|. \tag{40}$$

Similarly, one has

$$h(\mathbf{y}) = \log_2\left((\pi e)^K\left|\mathbf{C}_{\mathbf{y}}\right|\right) + \frac{1}{2}\log_2\left|\mathbf{I}_K - \mathbf{C}_{\mathbf{y}}^{-1}\tilde{\mathbf{C}}_{\mathbf{y}}\mathbf{C}_{\mathbf{y}}^{-\mathrm{T}}\tilde{\mathbf{C}}_{\mathbf{y}}^{\mathrm{H}}\right|. \tag{41}$$

The achievable rate can be obtained as [49]

$$\begin{aligned} C = I(\mathbf{x};\mathbf{y}) &= h(\mathbf{y}) - h(\mathbf{y}\mid\mathbf{x}) = h(\mathbf{y}) - h(\mathbf{z}) \\ &= \log_2\frac{\left|\mathbf{C}_{\mathbf{y}}\right|}{\left|\mathbf{C}_{\mathbf{z}}\right|} + \frac{1}{2}\log_2\frac{\left|\mathbf{I}_K - \mathbf{C}_{\mathbf{y}}^{-1}\tilde{\mathbf{C}}_{\mathbf{y}}\mathbf{C}_{\mathbf{y}}^{-\mathrm{T}}\tilde{\mathbf{C}}_{\mathbf{y}}^{\mathrm{H}}\right|}{\left|\mathbf{I}_K - \mathbf{C}_{\mathbf{z}}^{-1}\tilde{\mathbf{C}}_{\mathbf{z}}\mathbf{C}_{\mathbf{z}}^{-\mathrm{T}}\tilde{\mathbf{C}}_{\mathbf{z}}^{\mathrm{H}}\right|}. \end{aligned} \tag{42}$$

B. MIMO Radar Optimal SNR of Radar Receive Signal

Now we focus on the MIMO radar performance which maintains the necessary quality of the radar receive signal. Consider $\mathbf{M}_1\mathbf{x}+\mathbf{M}_2\mathbf{x}^*$ in (10) as the received radar information part and $\mathbf{K}_{r1}\mathbf{n}_0 + \mathbf{K}_{r2}\mathbf{n}_0^*$ in (10) as the noise part. From (10), the desired $\mathbf{w}$ is required to maximize the SNR of the MIMO radar as

$$\begin{aligned} \mathbf{w}_0 &= \arg\max_{\mathbf{w}}\frac{|\mathbf{w}^H\mathbf{M}_1\mathbf{x} + \mathbf{w}^H\mathbf{M}_2\mathbf{x}^*|^2}{\mathrm{E}(|\mathbf{w}^H\mathbf{K}_{r1}\mathbf{n}_0 + \mathbf{w}^H\mathbf{K}_{r2}\mathbf{n}_0^*|^2)} \\ &= \arg\max_{\mathbf{w}}\frac{\mathbf{w}^H(\mathbf{M}_1\mathbf{x}+\mathbf{M}_2\mathbf{x}^*)(\mathbf{M}_1\mathbf{x}+\mathbf{M}_2\mathbf{x}^*)^H\mathbf{w}}{\mathbf{w}^H(\mathbf{K}_{r1}\mathbf{K}_{r1}^H + \mathbf{K}_{r2}\mathbf{K}_{r2}^H)\mathbf{w}}. \end{aligned} \tag{43}$$

This is a typical Reighley quotient problem, which is equivalent to

$$\arg\max_{\mathbf{w}}\frac{\mathbf{w}^H[\mathbf{D}^{-\frac{1}{2}}(\mathbf{M}_1\mathbf{x}+\mathbf{M}_2\mathbf{x}^*)][\mathbf{D}^{-\frac{1}{2}}(\mathbf{M}_1\mathbf{x}+\mathbf{M}_2\mathbf{x}^*)]^H\mathbf{w}}{\mathbf{w}^H\mathbf{w}} \tag{44}$$

where $\mathbf{D} = \mathbf{K}_{r1}\mathbf{K}_{r1}^H + \mathbf{K}_{r2}\mathbf{K}_{r2}^H$. For a Reighlay quotient, one has

$$\begin{aligned} &\max_{\mathbf{w}}\frac{\mathbf{w}^H[\mathbf{D}^{-\frac{1}{2}}(\mathbf{M}_1\mathbf{x}+\mathbf{M}_2\mathbf{x}^*)][\mathbf{D}^{-\frac{1}{2}}(\mathbf{M}_1\mathbf{x}+\mathbf{M}_2\mathbf{x}^*)]^H\mathbf{w}}{\mathbf{w}^H\mathbf{w}} \\ &= (\mathbf{M}_1\mathbf{x}+\mathbf{M}_2\mathbf{x}^*)^H\mathbf{D}^{-1}(\mathbf{M}_1\mathbf{x}+\mathbf{M}_2\mathbf{x}^*). \end{aligned} \tag{45}$$

Thus, the corresponding optimal SNR of the MIMO radar is calculated as

$$\begin{aligned} \Lambda &= \mathrm{E}((\mathbf{M}_1\mathbf{x}+\mathbf{M}_2\mathbf{x}^*)^H\mathbf{D}^{-1}(\mathbf{M}_1\mathbf{x}+\mathbf{M}_2\mathbf{x}^*)) \\ &= \mathrm{E}[\mathrm{tr}((\mathbf{M}_1\mathbf{x}+\mathbf{M}_2\mathbf{x}^*)^H\mathbf{D}^{-1}(\mathbf{M}_1\mathbf{x}+\mathbf{M}_2\mathbf{x}^*))] \\ &= \mathrm{tr}(\mathbf{D}^{-1}(\mathbf{M}_1(\sum_{k=1}^K\mathbf{B}_k\mathbf{B}_k^H)\mathbf{M}_1^H + \mathbf{M}_2(\sum_{k=1}^K\mathbf{B}_k\mathbf{B}_k^H)^*\mathbf{M}_2^H)). \end{aligned} \tag{46}$$

C. Problem Formation and Solution

Therefore, the communication-centric optimization problem can be formulated as

$$\max_{\mathbf{B}_1,\ldots\mathbf{B}_K}\log_2\frac{|\mathbf{C}_{\mathbf{y}}|}{|\mathbf{C}_{\mathbf{z}}|} + \frac{1}{2}\log_2\frac{\left|\mathbf{I}_K - \mathbf{C}_{\mathbf{y}}^{-1}\tilde{\mathbf{C}}_{\mathbf{y}}\mathbf{C}_{\mathbf{y}}^{-\mathrm{T}}\tilde{\mathbf{C}}_{\mathbf{y}}^{\mathrm{H}}\right|}{\left|\mathbf{I}_K - \mathbf{C}_{\mathbf{z}}^{-1}\tilde{\mathbf{C}}_{\mathbf{z}}\mathbf{C}_{\mathbf{z}}^{-\mathrm{T}}\tilde{\mathbf{C}}_{\mathbf{z}}^{\mathrm{H}}\right|} \tag{47a}$$

$$\text{s.t. } \mathrm{tr}(\mathbf{D}^{-1}(\mathbf{M}_1(\sum_{k=1}^K\mathbf{B}_k\mathbf{B}_k^H)\mathbf{M}_1^H + \mathbf{M}_2(\sum_{k=1}^K\mathbf{B}_k\mathbf{B}_k^H)^*\mathbf{M}_2^H)) \geq \tau \tag{47b}$$

$$\mathrm{E}\left(\|\mathbf{x}_T\|^2\right) = \mathrm{tr}(\mathbf{G}_1(\sum_{k=1}^K\mathbf{B}_k\mathbf{B}_k^H)\mathbf{G}_1^* + \mathbf{G}_2^*(\sum_{k=1}^K\mathbf{B}_k\mathbf{B}_k^H)^*\mathbf{G}_2) \leq P_t \tag{47c}$$

where τ is the threshold on the MIMO radar SNR.

The problem in (47) is too complex to solve. Thus, we propose an alternative zero-forcing based beamforming scheme to reduce the complexity [50]. From (6), one sees both multi-user interference and IQI interference in the received signal. The key idea is to design the transmit beamforming to simultaneously eliminate the multi-user interference and IQI interference between different CUs. Thus, we have the additional constraints as

$$\begin{aligned} &\mathbf{h}_{1,i}^T\mathbf{B}_k = 0, \text{ for } i \neq k, \forall i,k \in \{1,\cdots,K\}, \\ &\mathbf{H}_2^T\mathbf{B}_k^* = \mathbf{0}, \forall k \in \{1,\cdots,K\} \Rightarrow \mathbf{H}_2^H\mathbf{B} = \mathbf{0}. \end{aligned} \tag{48}$$

Denote $\hat{\mathbf{H}}_k = [\mathbf{h}_{1,1},\cdots,\mathbf{h}_{1,k-1},\mathbf{h}_{1,k+1},\cdots,\mathbf{h}_{1,K},\mathbf{H}_2^*]^T \in \mathcal{C}^{(2K-1)\times N}$. From (48), one has

$$\hat{\mathbf{H}}_k\mathbf{B}_k = \mathbf{0}, \forall k \in \{1,\cdots,K\}. \tag{49}$$

Algorithm 2 Communication-Centric Optimization via ZF

1: Carry out SVD for the effective channel matrix as in (48)-(55).
2: Recompute the achievable sum rate as (57).
3: Establish the convex optimization problem as (59).
4: Solve (59) via the algorithm in [38].
5: Obtain $\hat{\mathbf{B}}_k$ for each k by (55).

Therefore, $\mathbf{B}_k$ is in the null space of $\hat{\mathbf{H}}_k$ which can be expressed as

$$\hat{\mathbf{H}}_k \overset{(a)}{=} \hat{\mathbf{U}}_k \hat{\Sigma}_k \left[\hat{\mathbf{V}}_k^{(1)}, \hat{\mathbf{V}}_k^{(0)}\right]^H \tag{50}$$

where (a) is from the singular value decomposition (SVD), $\hat{\mathbf{U}}_k \in \mathcal{C}^{(2K-1)\times(2K-1)}$ is a unitary matrix, $\hat{\Sigma}_k \in \mathcal{C}^{(2K-1)\times N} = \mathrm{diag}(a_{k,1}, ..., a_{k,\mathrm{rank}(\hat{\mathbf{H}}_k)})$, $\hat{\mathbf{V}}_k^{(0)} \in \mathcal{C}^{N\times(N-\mathrm{rank}(\hat{\mathbf{H}}_k))}$ forms an orthogonal basis consisting of $N-\mathrm{rank}(\hat{\mathbf{H}}_k)$ right singular vectors for the null space of $\hat{\mathbf{H}}_k$ and $\left[\hat{\mathbf{V}}_k^{(1)}, \hat{\mathbf{V}}_k^{(0)}\right] \in \mathcal{C}^{N\times N}$ is also a unitary matrix. Similarly, one has

$$\mathbf{h}_{1,k}^T \hat{\mathbf{V}}_k^{(0)} \overset{(a)}{=} \overline{\mathbf{U}}_k \overline{\mathbf{\Sigma}}_k \overline{\mathbf{V}}_k^H \in \mathcal{C}^{1\times(N-\mathrm{rank}(\hat{\mathbf{H}}_k))} \tag{51}$$

where $\overline{\mathbf{U}}_k = 1$ and $\overline{\mathbf{V}}_k \in \mathcal{C}^{(N-\mathrm{rank}(\hat{\mathbf{H}}_k))\times(N-\mathrm{rank}(\hat{\mathbf{H}}_k))}$ are unitary matrices, and $\overline{\Sigma}_k = \mathrm{diag}(h_k) \in \mathcal{C}^{1\times(N-\mathrm{rank}(\hat{\mathbf{H}}_k))}$. Then, the block diagonalization transmit beamforming can be used as

$$\mathbf{B}_k^{(\mathrm{BD})} = \hat{\mathbf{V}}_k^{(0)} \overline{\mathbf{V}}_k \mathbf{\Lambda}_k^{\frac{1}{2}} \tag{52}$$

where $\mathbf{\Lambda}_k = \mathrm{diag}(p_k) \in \mathcal{C}^{(N-\mathrm{rank}(\hat{\mathbf{H}}_k))\times 1}$. Denote $\hat{\mathbf{V}}_{\mathbf{k}}^{(\mathbf{0})} \overline{\mathbf{V}}_{\mathbf{k}} = [\mathbf{V}_{k,1}, ..., \mathbf{V}_{k,N-\mathrm{rank}(\hat{\mathbf{H}}_k)}]$ where $\mathbf{V}_{k,i} \in \mathcal{C}^{N\times 1}, \forall i$ and $\mathbf{V}_{k,i}^H \mathbf{V}_{k,i} = 1$. Using the above equations, one has

$$\mathbf{H}_1^T \mathbf{B} = \mathrm{diag}(h_1\sqrt{p_1}, ..., h_K\sqrt{p_K}), \tag{53}$$

$$\mathbf{H}_2^T \mathbf{B}^* = \mathbf{0} \tag{54}$$

and

$$\mathbf{B}_k^{(\mathrm{BD})} = \sqrt{p_k}\mathbf{V}_{k,1}. \tag{55}$$

Therefore, (36) becomes

$$\begin{cases} \tilde{\mathbf{C}}_{\mathbf{y}} = \tilde{\mathbf{C}}_{\mathbf{z}} \\ \mathbf{C}_{\mathbf{y}} = \mathrm{diag}(h_1^2 p_1, ..., h_K^2 p_K) + \mathbf{C}_{\mathbf{z}} \end{cases} \tag{56}$$

and (42) becomes

$$C = \frac{1}{2}\log_2 \frac{\prod_{k=1}^K (h_k^4 p_k^2 + (1+g_{R,k}^2)h_k^2 p_k + g_{R,k}^2 \cos^2\phi_{R,k})}{|\mathbf{C}_{\mathbf{z}}^2 - \tilde{\mathbf{C}}_{\mathbf{z}}\tilde{\mathbf{C}}_{\mathbf{z}}^*|} \tag{57}$$

where the detailed procedure is given in Appendix A. For $\mathbf{B}\mathbf{B}^H$, one has

$$\mathbf{B}\mathbf{B}^H = \sum_{k=1}^K \mathbf{B}_k^{(\mathrm{BD})}(\mathbf{B}_k^{(\mathrm{BD})})^H = \sum_{k=1}^K p_k \mathbf{V}_{k,1}\mathbf{V}_{k,1}^H. \tag{58}$$

Therefore, (47) is equivalent to the following concave problem (the detailed procedure is given in Appendix B) as

$$\max_{p_1,...,p_K} \sum_{k=1}^K \log_2(h_k^4 p_k^2 + (1+g_{R,k}^2)h_k^2 p_k + g_{R,k}^2 \cos^2\phi_{R,k}) \tag{59a}$$

$$\text{s.t. } \mathrm{tr}(\mathbf{D}^{-1}(\mathbf{M}_1(\sum_{k=1}^K \mathbf{B}_k\mathbf{B}_k^H)\mathbf{M}_1^H + \mathbf{M}_2(\sum_{k=1}^K \mathbf{B}_k\mathbf{B}_k^H)^*\mathbf{M}_2^H)) \geq r \times \Lambda_m \tag{59b}$$

$$-\mathrm{tr}(\mathbf{G}_1(\sum_{k=1}^K \mathbf{B}_k\mathbf{B}_k^H)\mathbf{G}_1^* + \mathbf{G}_2^*(\sum_{k=1}^K \mathbf{B}_k\mathbf{B}_k^H)^*\mathbf{G}_2) \geq -P_t \tag{59c}$$

$$\sum_{k=1}^K \mathbf{B}_k\mathbf{B}_k^H = \sum_{k=1}^K p_k \mathbf{V}_{k,1}\mathbf{V}_{k,1}^H. \tag{59d}$$

The computational complexity of SVD for the effective channel matrix of the k-th CU is $\mathcal{O}\left(N^3\right)$. The problem in (59) can be solved using the algorithm in [38] with dual-variable bisection search of $\max(L_1, L_2)$, where L_1 and L_2 are the number of iterations for the transmit power constraint and the MIMO radar receive SCNR constraint, respectively [38]. Therefore, the total computational complexity is $K\max(L_1, L_2)\mathcal{O}\left(N^3\right)$. By tuning r, one can obtain the solution to (59) at different levels of radar-communications tradeoff.

V. Numerical Results and Discussion

In this section, the performances of the proposed DFRC beamforming designs, i.e. the SDR radar-centric beamforming and zero-forcing communciation-centric beamforming, are evaluated via Monte Carlo simulation. These simulation results provide validation for the efficiency of the proposed beamforming approaches. In all experiments, the following settings are used unless specified otherwise. Both the DFRC BS and the MIMO radar receiver are equipped with uniform linear arrays (ULAs) with the same number of elements and half wavelength spacing between adjacent antennas. The total transmit SNR budget is set as $P_t = 30dB$. The multi-user communications channels are assumed to obey Rayleigh fading, so the elements of the channel matrices $\mathbf{H}$ are i.i.d. standard complex Gaussian random variables $\mathcal{CN}(0, 1, 0)$. The AWGN at each user and MIMO radar receiving antenna also has a variance of $\sigma^2 = 1$. For the ideal MIMO radar beampattern, the relevant parameters are set as main beam $\theta_0 = 0°$, $\theta_1 = 10°$, $\theta_2 = -10°$ and the sidelobe region $= [-90°, -20°] \cup [20°, 90°]$.

In the simulation, the number of communications users K and the number of antennas for DFRC BS N change to test their impact on the performance of the proposed joint beamforming approach. The amplitude mismatch $g_{T,i}$, $g_{R,i}$ and $g_{r,i}$ are uniformly generated from the common interval $g : [g_l, g_u]$ while the phase mismatch $\phi_{T,i}$, $\phi_{R,i}$ and $\phi_{r,i}$ are uniformly generated from the common interval $\phi : [\phi_l, \phi_u]$ (in this case BS and CUs have the symmetric IQI level). We tune the values of g_l, g_u, ϕ_l and ϕ_u to study the effect of IQI. Both problems involved in (28) and (59) are solved by using the MATLAB CVX toolbox. All the following simulation results are obtained by averaging over 1000 Monte Carlo runs.

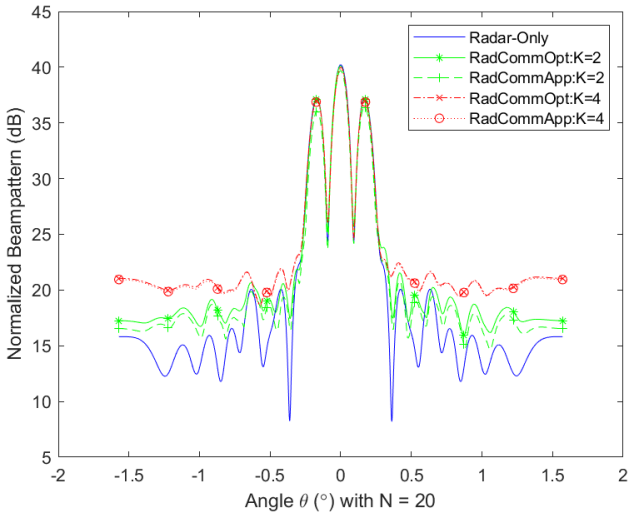

Fig. 1. Beampattern when $N = 20$ with $g_l = 0.95, g_u = 1, \phi_l = 0°$ and $\phi_u = 5°$.

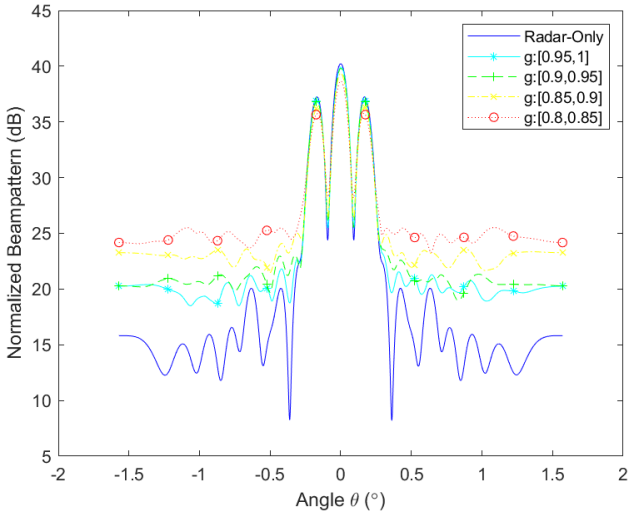

Fig. 2. Beampattern when $N = 20$ and $K = 4$ with $\phi_l = 0°$ and $\phi_u = 0°$.

A. Radar-Centric Transmit Beamforming

First, the proposed SDR transmit beamforming approach in (28) is studeied using the MIMO radar transmit beampatterns defined in (14). IQI parameters are set as $g_l = 0.95, g_u = 1, \phi_l = 0°$ and $\phi_u = 5°$. Communications SINR threshold Γ is chosen as $\frac{P_t}{\min\{K,10\}}$. The transmit beampatterns for $N = 20$ are depicted in Fig. 1 with $K = 0, 2$ or 4. When $K = 0$, it represents the radar-only beam pattern without any DFRC multi-users. Its beampattern has the overall best shape [43]. Such desired shape requires that the beam power in the mainlobe be extremely high and the beam power in the sidelobe be as low as possible, so that most transmit signal power is concentrated in the mainlobe to detect the target better. When $K = 2$, it is shown that the beam power of the mainlobe is smaller than that of 'Radar-Only' while the beam power of the sidelobe is much greater than that of 'Radar-Only'. From this perspective, adding two communications users degrades the beampattern performance of the MIMO radar-only system. When $K = 4$, the degradation is larger than that for $K = 2$. This phenomenon discloses the tradeoff that one cannot simultaneously achieve both optimal MIMO radar performance and optimal multiuser communications performance. This is the reason for choosing radar-centric or communication-centric architectures. 'RadarCommOpt' is the beampattern from (28) while 'RadarCommApp' is the beampattern from the approximation solution in (30) and (31). When $K = 2$, there is a slight mismatch between 'RadarCommApp' and 'RadarCommOpt'. However, when $K = 4$, the mismatch becomes quite smaller, which indicates the effectiveness of the proposed SDR beamforming solution in (30) and (31). This observation further validates the SDR beamforming approximation, when K is large enough.

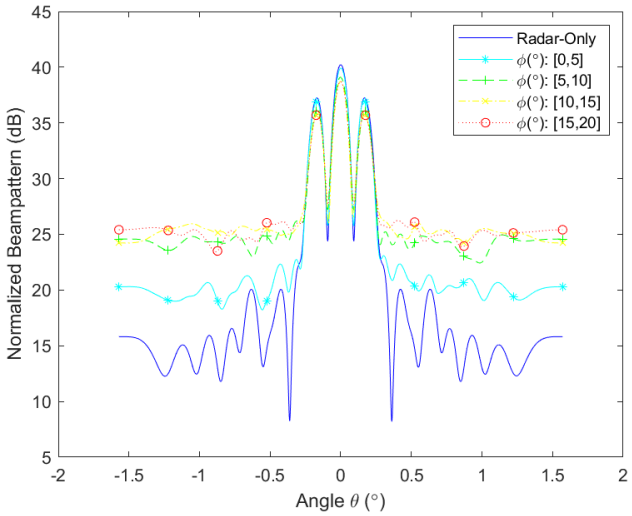

Fig. 3. Beampattern when $N = 20$ and $K = 4$ with $g_l = 1$ and $g_u = 1$.

In Fig.2, we fix $N = 20$, $K = 4$ and $\phi_l = \phi_u = 0°$ to explore amplitude mismatch's impact on DFRC system. Four intervals of $[g_l, g_u]$ are provided where a lower g_l and g_u stands for a more severe amplitude mismatch. The beampatterns of different amplitude mismatch levels are explicitly separated in Fig. 2. The greater amplitude mismatch is, the worse the beampattern will be. Therefore, amplitude mismatch has a degrading effect on the system performance. In Fig. 3, phase mismatch's impact on DFRC system is illustrated by fixing $N = 20$, $K = 4$ and $g_l = g_u = 1$. Similarly, it also has a degrading effect on the beampattern performance, though it is not as significant as that of the amplitude mismatch.

B. Communication-Centric Transmit Beamforming

In Fig. 4, the IQI parameters are specified as $g_l = 0.95, g_u = 1, \phi_l = 0°$ and $\phi_u = 5°$. Y axis is the communciations achievable rate C in (57) and X axis is the ratio threshold r of the DFRC radar SNR. Hence, we tune r to realize the tradeoff between communications performance and radar performance, since a bigger r reflects more consideration on the radar side. For all curves, C gradually decreases as r increases. Adding more communication users or more BS antennas will greatly increase the overall C. When $N = 10$, C decreases faster as K increases. However, increasing K

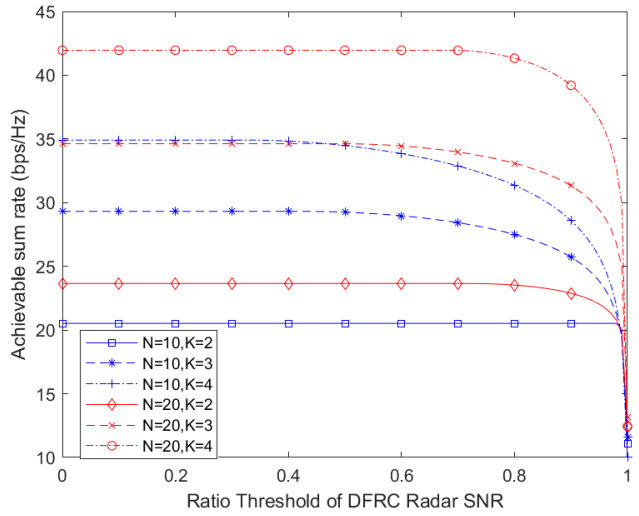

Fig. 4. Achievable rate when $N = 20$ and $K = 4$ with $g_l = 0.95, g_u = 1, \phi_l = 0°$ and $\phi_u = 5°$.

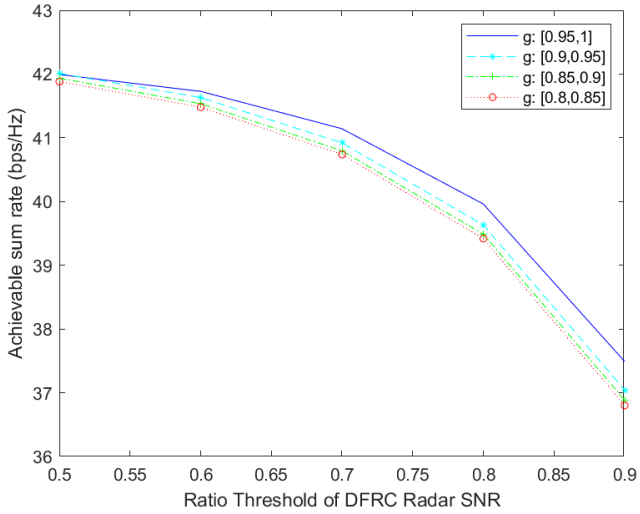

Fig. 5. Achievable rate when $N = 20$ and $K = 4$ with $\phi_l = 0°$ and $\phi_u = 0°$.

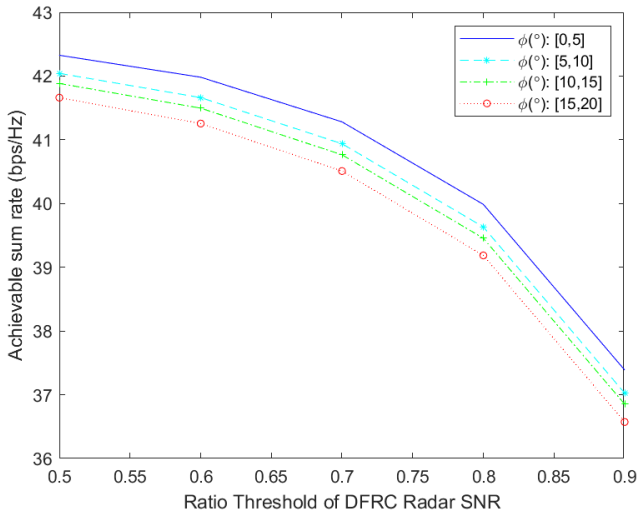

Fig. 6. Achievable rate when $N = 20$ and $K = 4$ with $g_l = 1$ and $g_u = 1$.

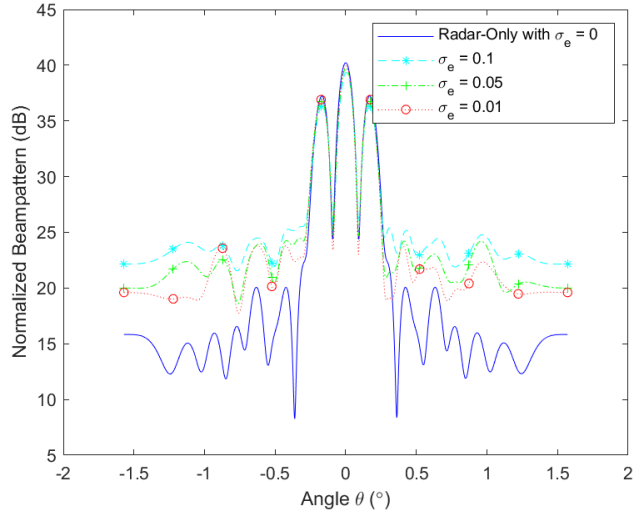

Fig. 7. Effect of IQI mitigation error on beampattern when $N = 20$ and $K = 4$ with $g_l = 0.95, g_u = 1, \phi_l = 0°$ and $\phi_u = 5°$.

does not significantly speed up C's decrease when $N = 20$, which means that it is useful to equip much more DFRC BS antennas to enhance the overall DFRC system performance. Fixing $N = 20$, $K = 4$ and $\phi_l = \phi_u = 0°$, we demonstrate amplitude mismatch's impact on the communication-centric DFRC system in Fig. 5 by using the same intervals of $[g_l, g_u]$ as Fig. 2. Each curve is explicitly separated and the achievable rate decreases as the amplitude mismatch gets more severe. In Fig. 6, phase mismatch is also found to have a degrading effect on the communications achievable rate performance. Fig. 2, Fig. 3, Fig. 5 and Fig. 6 show that IQI is of critical importance to be considered and compensated for improving future MIMO DFRC system performance.

C. Further Impact of the IQI

In the above, IQI is perfectly known. However, in many realistic scenarios, it is difficult to obtain an accurate value of IQI. Alternatively, IQI mitigation methods could be utilized. For each diagonal element of the IQI matrices $\mathbf{K}_1$, $\mathbf{K}_{r1}$ and $\mathbf{G}_1$, its estimation error is assumed to be complex Gaussian with $\mathcal{CN}(0, \sigma_e^2, 0)$, where σ_e^2 is the error variance. Here, σ_e is set as 0.1, 0.05 or 0.01 to study the impact of imperfect IQI mitigation on both radar-centric DFRC beamforming and communication-centric DFRC beamforming. Other relevant parameters are $N = 20$, $K = 4$, $g_l = 0.95, g_u = 1, \phi_l = 0°$ and $\phi_u = 5°$. In Fig. 7, one finds that the beampattern is compromised as σ_e increases. Similarly, in Fig. 8 the achievable rate decreases when the error variance increases. These results show the importance of achieving accurate and efficient IQI mitigation. Next, the case when the BS and CUs have asymmetric IQI levels is studied. The amplitude mismatches at the BS $g_{T,i}$ and $g_{r,i}$ are uniformly generated from the interval $g_b : [g_{bl}, g_{bu}]$ while the amplitude mismatch at the CU $g_{R,i}$ is uniformly generated from the interval $g_c : [g_{cl}, g_{cu}]$. Also, the phase mismatches at the BS $\phi_{T,i}$ and $\phi_{r,i}$ are uniformly generated from the interval $\phi_b : [\phi_{bl}, \phi_{bu}]$ while the phase mismatch at the CU $\phi_{R,i}$ is uniformly generated

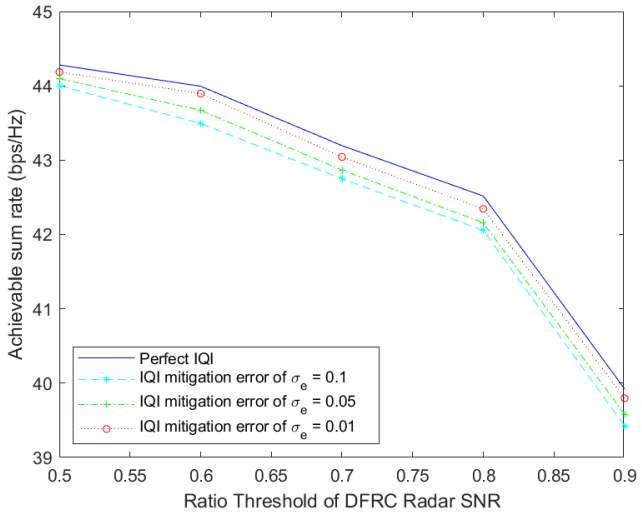

Fig. 8. Effect of IQI mitigation error on achievable rate when $N = 20$ and $K = 4$ with $g_l = 0.95, g_u = 1, \phi_l = 0°$ and $\phi_u = 5°$.

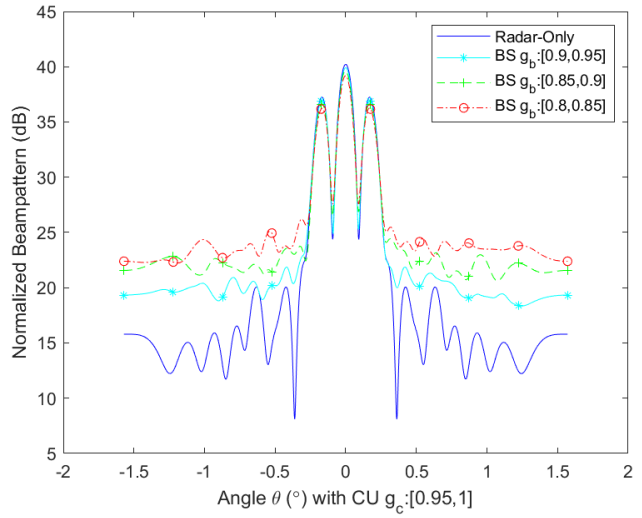

Fig. 9. Effect of asymmetric amplitude mismatch level on beampattern when $N = 20$ and $K = 4$ with $\phi_b(°) = \phi_c(°) = [0, 0]$.

from the interval $\phi_c : [\phi_{cl}, \phi_{cu}]$. For the radar-centric scenario, we set $\phi_b(°) = \phi_c(°) = [0, 0]$ and fix $g_c = [0.95, 1]$ to explore the effect of aymmetric level of g_b. Fig. 9 shows that the amplitude mismatch still has a significant impact on the radar beampattern performance. For the communication-centric scenario, we set $g_b = g_c = [1, 1]$ to explore the effect of aymmetric level of ϕ_b and ϕ_c. From Fig. 10, one sees that the overall achievable rate improves as ϕ_c gets better while ϕ_b gets worse. This interesting result indicates that the phase mismatch at the CU side has much more significant impact than that at the BS side.

D. System Analysis

Radar-centric and communications-centric are two different perspectives of optimization for DFRC. One can also carry out the joint optimization by constructing the weighted sum of the radar performance and the communications performance.

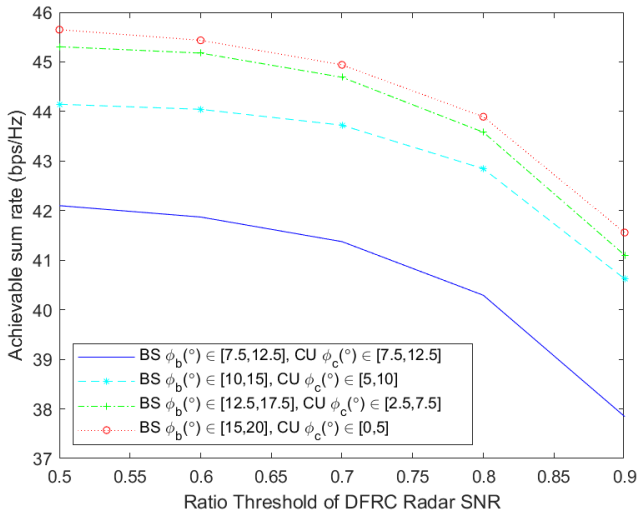

Fig. 10. Effect of asymmetric phase mismatch level on achievable rate when $N = 20$ and $K = 4$ with $g_b = g_c = [1, 1]$.

This might provide more insights to improve the overall performance of DFRC. Also, new transmit beamforming for the emerging ultra-massive MIMO communications is interesting. For the CUs, this work can be extended to the multi-antenna case. Also, for multiple radar targets with high mobility, the DFRC system must consider the Doppler effect, return signal time delay and clutter interference. Finally, other HWI types can be investigated.

VI. Conclusion

In this work, we have extended the conventional DFRC beamforming designs to a more realistic scenario considering the existence of IQI. In order to achieve the optimal DFRC performance, both radar-centric and communication-centric optimizations have been proposed. For the radar-centric formulation, the beampattern design under constraints of mainlobe beam power, sidelobe beam power and each communications user's minimum SINR has been proposed. SDR has been employed to obtain a good approximation. For the communication-centric beamforming design, zero-forcing based approach has been proposed to greatly reduce the computation complexity. IQI amplitude mismatch, IQI phase mismatch and IQI mitigation error have been shown to have significant effect on the overall performance. For the communication-centric scenario, IQI phase mismatch at the CUs has more significant impact than IQI phase mismatch at the BS. Therefore, future massive MIMO DFRC system shall consider mitigating IQI and improve the IQI estimation accuracy.

Appendix

A. Derivation of the Achievable Sum Rate

From (34), (35) and (56), one finds that the multiplications of $\mathbf{C_y}$, $\tilde{\mathbf{C}}_\mathbf{y}$, $\mathbf{C_z}$ and $\tilde{\mathbf{C}}_\mathbf{z}$ are commutative since all of them are

diagonal matrices of the same order. Therefore, one has

$$\begin{aligned} C &= \log_2 \frac{|\mathbf{C_y}|}{|\mathbf{C_z}|} + \frac{1}{2}\log_2 \frac{\left|\mathbf{I}_K - \mathbf{C_y}^{-1}\tilde{\mathbf{C}}_\mathbf{y}\tilde{\mathbf{C}}_\mathbf{y}^{\mathrm{H}}\mathbf{C_y}^{-\mathrm{T}}\right|}{\left|\mathbf{I}_K - \mathbf{C_z}^{-1}\tilde{\mathbf{C}}_\mathbf{z}\mathbf{C_z}^{-\mathrm{T}}\tilde{\mathbf{C}}_\mathbf{z}^{\mathrm{H}}\right|} \\ &= \frac{1}{2}\log_2 \frac{|\mathbf{C_y}|^2\left|\mathbf{I}_K - \mathbf{C_y}^{-1}\tilde{\mathbf{C}}_\mathbf{y}\tilde{\mathbf{C}}_\mathbf{y}^{\mathrm{H}}\mathbf{C_y}^{-\mathrm{T}}\right|}{|\mathbf{C_z}|^2\left|\mathbf{I}_K - \mathbf{C_z}^{-1}\tilde{\mathbf{C}}_\mathbf{z}\tilde{\mathbf{C}}_\mathbf{z}^{\mathrm{H}}\mathbf{C_z}^{-\mathrm{T}}\right|} \\ &= \frac{1}{2}\log_2 \frac{|\mathbf{C_y^2} - \tilde{\mathbf{C}}_\mathbf{y}\tilde{\mathbf{C}}_\mathbf{y}^{*}|}{|\mathbf{C_z^2} - \tilde{\mathbf{C}}_\mathbf{z}\tilde{\mathbf{C}}_\mathbf{z}^{*}|} \\ &= \frac{1}{2}\log_2 \frac{|\mathbf{C_y^2} - \tilde{\mathbf{C}}_\mathbf{z}\tilde{\mathbf{C}}_\mathbf{z}^{*}|}{|\mathbf{C_z^2} - .\tilde{\mathbf{C}}_\mathbf{z}\tilde{\mathbf{C}}_\mathbf{z}^{*}|}. \end{aligned} \tag{60}$$

The k-th diagonal elements of $\mathbf{C_y^2}$ and $\tilde{\mathbf{C}}_\mathbf{z}\tilde{\mathbf{C}}_\mathbf{z}^{*}$ are $(h_k^2 p_k + \frac{1+g_{R,k}^2}{2})^2$ and $\frac{1+g_{R,k}^4-2g_{R,k}^2+4g_{R,k}^2\sin^2\phi_{R,k}}{4}$, respectively, after quantities sustitution and calculation. Therefore, one finally has (57).

B. Formation of the Communication-Centric Problem

If (57) and (58) are obtained by the zero-forcing method, the problem in (47) becomes a power allocation problem:

$$\max_{p_1,\ldots,p_K} \sum_{k=1}^{K} \log_2(h_k^4 p_k^2 + (1+g_{R,k}^2)h_k^2 p_k + g_{R,k}^2\cos^2\phi_{R,k}) \tag{61a}$$

$$\text{s.t. } \mathrm{tr}(\mathbf{D}^{-1}(\mathbf{M}_1(\sum_{k=1}^{K}\mathbf{B}_k\mathbf{B}_k^H)\mathbf{M}_1^H + \mathbf{M}_2(\sum_{k=1}^{K}\mathbf{B}_k\mathbf{B}_k^H)^*\mathbf{M}_2^H)) \tag{61b}$$

$$\geq \tau$$

$$\mathrm{tr}(\mathbf{G}_1(\sum_{k=1}^{K}\mathbf{B}_k\mathbf{B}_k^H)\mathbf{G}_1^* + \mathbf{G}_2^*(\sum_{k=1}^{K}\mathbf{B}_k\mathbf{B}_k^H)^*\mathbf{G}_2) \leq P_t \tag{61c}$$

$$\sum_{k=1}^{K}\mathbf{B}_k\mathbf{B}_k^H = \sum_{k=1}^{K} p_k\mathbf{V}_{k,1}\mathbf{V}_{k,1}^H. \tag{61d}$$

Since both the left side of (61b) and the right side of (61d) are linear with of $p_1, ..., p_K$, one has the following ancillary concave optimization problem:

$$\max_{p_1,\ldots,p_K} \mathrm{tr}(\mathbf{D}^{-1}(\mathbf{M}_1(\sum_{k=1}^{K}\mathbf{B}_k\mathbf{B}_k^H)\mathbf{M}_1^H + \mathbf{M}_2(\sum_{k=1}^{K}\mathbf{B}_k\mathbf{B}_k^H)^*\mathbf{M}_2^H)) \tag{62a}$$

$$\text{s.t. } -\mathrm{tr}(\mathbf{G}_1(\sum_{k=1}^{K}\mathbf{B}_k\mathbf{B}_k^H)\mathbf{G}_1^* + \mathbf{G}_2^*(\sum_{k=1}^{K}\mathbf{B}_k\mathbf{B}_k^H)^*\mathbf{G}_2) \geq -P_t \tag{62b}$$

$$\sum_{k=1}^{K}\mathbf{B}_k\mathbf{B}_k^H = \sum_{k=1}^{K} p_k\mathbf{V}_{k,1}\mathbf{V}_{k,1}^H, \tag{62c}$$

whose maximum objective value is denoted as Λ_m. Therefore, (61b) can be rewritten as

$$\mathrm{tr}(\mathbf{D}^{-1}(\mathbf{M}_1(\sum_{k=1}^{K}\mathbf{B}_k\mathbf{B}_k^H)\mathbf{M}_1^H + \mathbf{M}_2(\sum_{k=1}^{K}\mathbf{B}_k\mathbf{B}_k^H)^*\mathbf{M}_2^H)) \geq r\times\Lambda_m \tag{63}$$

where r is the ratio threshold of DFRC radar SNR in $[0, 1]$. For (61a), denoting $\log_2(h_k^4p_k^2 + (1+g_{R,k}^2)h_k^2p_k + g_{R,k}^2\cos^2\phi_{R,k})$ as $f_k(p_k)$, one has

$$f_k^{'}(p_k) = \frac{2h_k^4p_k + (1+g_{R,k}^2)h_k^2}{h_k^4p_k^2 + (1+g_{R,k}^2)h_k^2p_k + g_{R,k}^2\cos^2\phi_{R,k}} > 0 \tag{64}$$

and

$$\begin{aligned} &f_k^{''}(p_k) = \\ &-\frac{h_k^4(2h_k^4p_k^2 + 2(1+g_{R,k}^2)h_k^2p_k + g_{R,k}^4 + 2g_{R,k}^2\sin^2\phi_{R,k} + 1)}{(h_k^4p_k^2 + (1+g_{R,k}^2)h_k^2p_k + g_{R,k}^2\cos^2\phi_{R,k})^2} \\ &< 0. \end{aligned} \tag{65}$$

Therefore, $f_k(p_k)$ is a concave function so (61a) is also concave. Then, one has the equivalent communication-centric problem as (59).

REFERENCES

[1] W. Saad, M. Bennis, and M. Chen, "A vision of 6g wireless systems: Applications, trends, technologies, and open research problems," *IEEE network*, vol. 34, no. 3, pp. 134–142, 2019.

[2] L. Zheng, M. Lops, Y. C. Eldar, and X. Wang, "Radar and communication coexistence: An overview: A review of recent methods," *IEEE Signal Processing Magazine*, vol. 36, no. 5, pp. 85–99, 2019.

[3] F. Liu, C. Masouros, A. Li, H. Sun, and L. Hanzo, "Mu-mimo communications with mimo radar: From co-existence to joint transmission," *IEEE Transactions on Wireless Communications*, vol. 17, no. 4, pp. 2755–2770, 2018.

[4] F. Liu, L. Zhou, C. Masouros, A. Li, W. Luo, and A. Petropulu, "Toward dual-functional radar-communication systems: Optimal waveform design," *IEEE Transactions on Signal Processing*, vol. 66, no. 16, pp. 4264–4279, 2018.

[5] A. Hassanien, M. G. Amin, Y. D. Zhang, and F. Ahmad, "Dual-function radar-communications: Information embedding using sidelobe control and waveform diversity," *IEEE Transactions on Signal Processing*, vol. 64, no. 8, pp. 2168–2181, 2015.

[6] M. F. Keskin, V. Koivunen, and H. Wymeersch, "Limited feedforward waveform design for ofdm dual-functional radar-communications," *IEEE Transactions on Signal Processing*, vol. 69, pp. 2955–2970, 2021.

[7] F. Liu, C. Masouros, T. Ratnarajah, and A. Petropulu, "On range sidelobe reduction for dual-functional radar-communication waveforms," *IEEE Wireless Communications Letters*, vol. 9, no. 9, pp. 1572–1576, 2020.

[8] X. Wang, Z. Fei, Z. Zheng, and J. Guo, "Joint waveform design and passive beamforming for ris-assisted dual-functional radar-communication system," *IEEE Transactions on Vehicular Technology*, vol. 70, no. 5, pp. 5131–5136, 2021.

[9] A. Bazzi and M. Chafii, "On outage-based beamforming design for dual-functional radar-communication 6g systems," *arXiv preprint arXiv:2207.04921*, 2022.

[10] Z. Cheng, Z. He, and B. Liao, "Hybrid beamforming design for ofdm dual-function radar-communication system," *IEEE Journal of Selected Topics in Signal Processing*, vol. 15, no. 6, pp. 1455–1467, 2021.

[11] Z. Cheng and B. Liao, "Qos-aware hybrid beamforming and doa estimation in multi-carrier dual-function radar-communication systems," *IEEE Journal on Selected Areas in Communications*, vol. 40, no. 6, pp. 1890–1905, 2022.

[12] C. Qi, W. Ci, J. Zhang, and X. You, "Hybrid beamforming for millimeter wave mimo integrated sensing and communications," *IEEE Communications Letters*, vol. 26, no. 5, pp. 1136–1140, 2022.

[13] Y. Li and M. Jiang, "Joint transmit beamforming and receive filters design for coordinated two-cell interfering dual-functional radar-communication networks," *IEEE Transactions on Vehicular Technology*, 2022.

[14] T. Huang, N. Shlezinger, X. Xu, Y. Liu, and Y. C. Eldar, "Majorcom: A dual-function radar communication system using index modulation," *IEEE transactions on signal processing*, vol. 68, pp. 3423–3438, 2020.

[15] N. Su, F. Liu, Z. Wei, Y.-F. Liu, and C. Masouros, "Secure dual-functional radar-communication transmission: Exploiting interference for resilience against target eavesdropping," *IEEE Transactions on Wireless Communications*, vol. 21, no. 9, pp. 7238–7252, 2022.

[16] Z. Yang, D. Li, N. Zhao, Z. Wu, Y. Li, and D. Niyato, "Secure precoding optimization for noma-aided integrated sensing and communication," *IEEE Transactions on Communications*, vol. 70, no. 12, pp. 8370–8382, 2022.
[17] F. Dong, W. Wang, X. Li, F. Liu, S. Chen, and L. Hanzo, "Joint beamforming design for dual-functional mimo radar and communication systems guaranteeing physical layer security," *IEEE Transactions on Green Communications and Networking*, 2023.
[18] F. Liu, W. Yuan, C. Masouros, and J. Yuan, "Radar-assisted predictive beamforming for vehicular links: Communication served by sensing," *IEEE Transactions on Wireless Communications*, vol. 19, no. 11, pp. 7704–7719, 2020.
[19] B. Liu, J. Liu, and N. Kato, "Optimal beamformer design for millimeter wave dual-functional radar-communication based v2x systems," *IEEE Journal on Selected Areas in Communications*, vol. 40, no. 10, pp. 2980–2993, 2022.
[20] X. Chen, Z. Feng, Z. Wei, F. Gao, and X. Yuan, "Performance of joint sensing-communication cooperative sensing uav network," *IEEE Transactions on Vehicular Technology*, vol. 69, no. 12, pp. 15 545–15 556, 2020.
[21] C. Ding, J.-B. Wang, H. Zhang, M. Lin, and G. Y. Li, "Joint mimo precoding and computation resource allocation for dual-function radar and communication systems with mobile edge computing," *IEEE Journal on Selected Areas in Communications*, 2022.
[22] Z.-M. Jiang, M. Rihan, P. Zhang, L. Huang, Q. Deng, J. Zhang, and E. M. Mohamed, "Intelligent reflecting surface aided dual-function radar and communication system," *IEEE Systems Journal*, vol. 16, no. 1, pp. 475–486, 2021.
[23] X. Wang, Z. Fei, Z. Zheng, and J. Guo, "Joint waveform design and passive beamforming for ris-assisted dual-functional radar-communication system," *IEEE Transactions on Vehicular Technology*, vol. 70, pp. 5131–5136, 2021.
[24] S. Javed, O. Amin, S. S. Ikki, and M.-S. Alouini, "Asymmetric modulation for hardware impaired systems—error probability analysis and receiver design," *IEEE Transactions on Wireless Communications*, vol. 18, no. 3, pp. 1723–1738, 2019.
[25] M. Mokhtar, A. Gomaa, and N. Al-Dhahir, "Ofdm af relaying under i/q imbalance: Performance analysis and baseband compensation," *IEEE Transactions on Communications*, vol. 61, no. 4, pp. 1304–1313, 2013.
[26] J. Li, M. Matthaiou, and T. Svensson, "I/q imbalance in af dual-hop relaying: Performance analysis in nakagami-m fading," *IEEE Transactions on Communications*, vol. 62, no. 3, pp. 836–847, 2014.
[27] Y. Gao, Y. Chen, N. Chen, and J. Zhang, "Performance analysis of dual-hop relaying with i/q imbalance and additive hardware impairment," *IEEE Transactions on Vehicular Technology*, vol. 69, no. 4, pp. 4580–4584, 2020.
[28] X. Huang, A. T. Le, and Y. J. Guo, "Joint analog and digital self-interference cancellation for full duplex transceiver with frequency-dependent i/q imbalance," *IEEE Transactions on Wireless Communications*, 2022.
[29] R. Zayani, H. Shaïek, and D. Roviras, "Efficient precoding for massive mimo downlink under pa nonlinearities," *IEEE Communications Letters*, vol. 23, pp. 1611–1615, 2019.
[30] Z. Mokhtari and R. Dinis, "Sum-rate of cell free massive mimo systems with power amplifier non-linearity," *IEEE Access*, vol. PP, pp. 1–1, 2021.
[31] P. Zhang, J. Liu, Y. Shen, and X. Jiang, "Exploiting channel gain and phase noise for phy-layer authentication in massive mimo systems," *IEEE Transactions on Information Forensics and Security*, vol. 16, pp. 4265–4279, 2021.
[32] H. Iimori, G. T. F. deAbreu, D. G. G., and O. Gonsa, "Mitigating channel aging and phase noise in millimeter wave mimo systems," *IEEE Transactions on Vehicular Technology*, vol. 70, pp. 7237–7242, 2021.
[33] C. Shan, Y. Zhang, L. Chen, X. Chen, and W. Wang, "Performance analysis of large scale antenna system with carrier frequency offset, quasi-static mismatch and channel estimation error," *IEEE Access*, vol. 5, pp. 26 135–26 145, 2017.
[34] Z. Mokhtari, M. Sabbaghian, and R. Dinis, "Massive mimo downlink based on single carrier frequency domain processing," *IEEE Transactions on Communications*, vol. 66, pp. 1164–1175, 2018.
[35] F. Kaltenberger, H. Jiang, M. Guillaud, and R. Knopp, "Relative channel reciprocity calibration in mimo/tdd systems," in *2010 Future Network & Mobile Summit*. IEEE, 2010, pp. 1–10.
[36] Y. Nan, L. Zhang, and X. Sun, "Efficient downlink channel estimation scheme based on block-structured compressive sensing for tdd massive mu-mimo systems," *IEEE Wireless Communications Letters*, vol. 4, no. 4, pp. 345–348, 2015.
[37] L. Xu, J. Li, and P. Stoica, "Target detection and parameter estimation for mimo radar systems," *IEEE Transactions on Aerospace and Electronic Systems*, vol. 44, no. 3, pp. 927–939, 2008.
[38] L. Chen, Z. Wang, Y. Du, Y. Chen, and F. R. Yu, "Generalized transceiver beamforming for dfrc with mimo radar and mu-mimo communication," *IEEE Journal on Selected Areas in Communications*, vol. 40, no. 6, pp. 1795–1808, 2022.
[39] M. A. Jensen and J. W. Wallace, "A review of antennas and propagation for mimo wireless communications," *IEEE Transactions on Antennas and propagation*, vol. 52, no. 11, pp. 2810–2824, 2004.
[40] A. M. Haimovich, R. S. Blum, and L. J. Cimini, "Mimo radar with widely separated antennas," *IEEE signal processing magazine*, vol. 25, no. 1, pp. 116–129, 2007.
[41] L. Zheng, M. Lops, Y. C. Eldar, and X. Wang, "Radar and communication coexistence: An overview: A review of recent methods," *IEEE Signal Processing Magazine*, vol. 36, no. 5, pp. 85–99, 2019.
[42] X. Liu, T. Huang, N. Shlezinger, Y. Liu, J. Zhou, and Y. C. Eldar, "Joint transmit beamforming for multiuser mimo communications and mimo radar," *IEEE Transactions on Signal Processing*, vol. 68, pp. 3929–3944, 2020.
[43] P. Stoica, J. Li, and Y. Xie, "On probing signal design for mimo radar," *IEEE Transactions on Signal Processing*, vol. 55, no. 8, pp. 4151–4161, 2007.
[44] N. Kolomvakis, M. Coldrey, T. Eriksson, and M. Viberg, "Massive mimo systems with iq imbalance: Channel estimation and sum rate limits," *IEEE Transactions on Communications*, vol. 65, no. 6, pp. 2382–2396, 2017.
[45] M. Grant and S. Boyd, "Cvx: Matlab software for disciplined convex programming, version 2.1," 2014.
[46] M. C. Grant and S. P. Boyd, "Graph implementations for nonsmooth convex programs," in *Recent advances in learning and control*. Springer, 2008, pp. 95–110.
[47] P. J. Schreier and L. L. Scharf, *Statistical signal processing of complex-valued data: the theory of improper and noncircular signals*. Cambridge university press, 2010.
[48] Y. Zeng, C. M. Yetis, E. Gunawan, Y. L. Guan, and R. Zhang, "Transmit optimization with improper gaussian signaling for interference channels," *IEEE Transactions on Signal Processing*, vol. 61, no. 11, pp. 2899–2913, 2013.
[49] S. Javed, O. Amin, S. S. Ikki, and M.-S. Alouini, "On the achievable rate of hardware-impaired transceiver systems," in *GLOBECOM 2017-2017 IEEE Global Communications Conference*. IEEE, 2017, pp. 1–6.
[50] Q. H. Spencer, A. L. Swindlehurst, and M. Haardt, "Zero-forcing methods for downlink spatial multiplexing in multiuser mimo channels," *IEEE transactions on signal processing*, vol. 52, no. 2, pp. 461–471, 2004.

Junqiu Wang received the B.E. in mathematics and applied mathematics from Shandong University, Weihai, China, in 2015 and the M.E. degree in probability theory and mathematical statistics from Xiamen University, Xiamen, China, in 2019. He is currently pursuing his PhD degree for electronics engineering with the School of Engineering, University of Warwick, UK. His research interests include joint communication and radar, hardware impairment, signal processing, autonomous driving and AI for 6G.

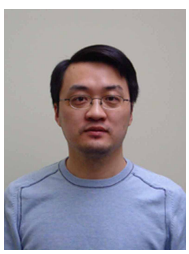

Yunfei Chen (S'02-M'06-SM'10) received his B.E. and M.E. degrees in electronics engineering from Shanghai Jiaotong University, Shanghai, P.R.China, in 1998 and 2001, respectively. He received his Ph.D. degree from the University of Alberta in 2006. He is currently working as a Professor at the University of Durham, U.K. His research interests include wireless communications, cognitive radios, wireless relaying and energy harvesting.

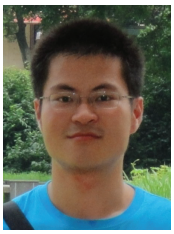

Li Chen received the B.E. in electrical and information engineering from Harbin Institute of Technology, Harbin, China, in 2009 and the Ph.D. degree in electrical engineering from the University of Science and Technology of China, Hefei, China, in 2014. He is currently an Associate Professor with the Department of Electronic Engineering and Information Science, University of Science and Technology of China. His research interests include integrated communication and computation and integrated communication and sensing.